Doppler Positioning with Orientation Estimation by Using Multiple Transmitters for High-accuracy IMES Localization

Yoshihiro Sakamoto and Shigeki Sugano
Dept. of Modern Mechanical Engineering
Waseda University
Tokyo, Japan

Takuji Ebinuma
Dept. of Aeronautics and Astronautics
The University of Tokyo
Tokyo, Japan

Kenjiro Fujii
Hitachi Industrial Equipment Systems Co., Ltd.
Tokyo, Japan

***Abstract*—A Doppler positioning method with orientation estimation for an indoor messaging system (IMES) is proposed. With this method, both position and orientation of a receiver are estimated simultaneously by using Doppler shifts produced by moving a receiver antenna under the use of two or more IMES transmitters. The proposed method is evaluated through an experiment in which the interval of two transmitters is varied. The results of the experiment demonstrate that centimeter- to decimeter-level positioning accuracy and orientation-estimation accuracy of ±3 degrees are achieved; these results were largely consistent with the theoretical values calculated from dilution of precision. In addition, magnetic-compass error indoors was experimentally investigated; the results show that a magnetic-compass is a large error source if it is used indoors. Lastly, which initial values of a nonlinear least-square used for the proposed method converge to appropriate position and orientation solutions is analyzed; the results of the analysis suggest that if an initial position is set to the midmost of two transmitters, a proper solution is obtained except in the case that initial orientation is 180 degrees opposite from the correct orientation.**

Keywords- Indoor Positioning, IMES, Doppler Positioning

I. INTRODUCTION

Presently, the Japanese government and Japan Aerospace Exploration Agency (JAXA) are promoting development of an indoor positioning system called "indoor messaging system" (IMES), which is proposed as a part of the quasi-zenith satellite system (QZSS) [1]. IMES is a ground-based GPS augmentation system that transmits a GPS-compatible signal, which is composed of a C/A code modulated on an L1-band carrier. Unlike GPS, IMES does not use trilateration; instead, its transmitter sends position information assigned to itself, and its receiver simply decodes the position from the transmitted signal [2]. In this method, the receiver can know its position if at least one transmitter is visible. Thanks to this simplicity, the position of the receiver can be stably obtained indoors, where the signal condition is basically worse than that outdoors because of multipaths and interference. This is a significant advantage compared to a conventional ground-based GPS augmentation system with pseudolites [3][4], which use range measurement and trilateration like GPS. As for the primary drawback of IMES, however, its positioning accuracy equals the installation interval between its transmitters (normally 10-20 meters). This accuracy is not a problem in the case that IMES is used for location-based services for people; however, in fields such as logistics management, tracking vehicles, and robot navigation, which require higher positioning accuracy, IMES cannot be directly used.

In our previous work, a method called Doppler positioning—which achieves centimeter- to decimeter-level positioning accuracy with IMES—was proposed [5]. Combined with a three-dimensional attitude sensor (including a three-axis accelerometer, a three-axis gyroscope, and a three-axis magnetometer), this method uses a Doppler shift (produced by moving a receiver antenna) for positioning. In a positioning experiment using a single IMES transmitter, centimeter- to decimeter-level positioning accuracy was achieved under the assumption that orientation (azimuth) errors due to both the magnetometer (magnetic compass) and magnetic declination (difference between the angles of magnetic north and Earth's true north) are zero. As can be easily imagined, especially a magnetic compass is a large error source when it is used indoors, where there are a lot of electric devices and iron-based materials that significantly influence local magnetic field.

In the present work, Doppler positioning is improved so that the above-mentioned orientation error can be avoided; that is, the position and orientation of the receiver are estimated at the same time by using multiple IMES transmitters.

978-1-4673-1954-6/12/$31.00 ©2012 IEEE

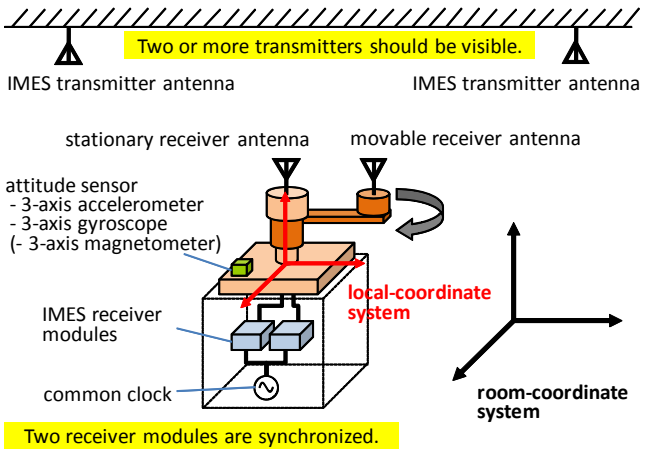

Figure 1. Overview of Doppler positioning with orientation estimation.

II. Doppler Positioning with Orientation Estimation

A. Overview

An overview of Doppler positioning with orientation estimation is given in Fig. 1. First, two types of coordinate system are defined: a local-coordinate system (LCS) and a room-coordinate system (RCS). The RCS is arbitrarily defined for each room and building, and the positions of the IMES transmitters are defined with respect to the RCS. To accomplish indoor-outdoor seamless positioning, the RCS must be convertible or identical to a global coordinate system such as "earth-centered earth-fixed" (ECEF) or "local-east, north-up" (ENU), which can be used anywhere on Earth. One axis of the RCS basically should be parallel with the direction of gravity because an accelerometer fitted in the attitude sensor is used to detect the inclination of the receiver. The LCS is fixed to the receiver. In the LCS, the position and velocity of the movable receiver antenna are known.

The primary difference between the proposed method and the previous Doppler positioning method [5] is that orientation (azimuth) information output from the attitude sensor and magnetic declination obtained from an external source (such as government websites) are not necessarily used for the positioning with the proposed method because the position and orientation of the receiver can be determined by using two or more transmitters. Since the proposed method has backward compatibility with the previous Doppler positioning method, if the number of visible transmitter becomes one, it can be switched to the previous one; moreover, the orientation estimated with the proposed method can be used for the previous one by holding it with a gyroscope or wheel encoders.

The positioning procedure is described as follows. First, when the receiver antenna is moved, Doppler shifts arise for each carrier wave from multiple transmitters. To obtain the Doppler shifts, two synchronized receiver modules are used: one is connected to a stationary antenna, and the other is connected to a movable antenna (see Fig. 1). By subtracting the output of the stationary receiver from that of the movable one, the clock biases of the transmitters and receivers are cancelled; accordingly, the Doppler shifts produced by the movement of the movable antenna are extracted. Meanwhile, the movable antenna's position and velocity with respect to the LCS are acquired from the encoder attached to the rotation axis, and the inclination of the receiver is obtained from the attitude sensor (equipped with a three-axis accelerometer). These variables are obtained while the movable antenna is rotating several round trips (rotating around the stationary antenna several times) and the position and orientation of the receiver with respect to the RCS are then calculated by using nonlinear least squares.

B. Acquision of Doppler shifts

Normally, as an observable, a GPS/IMES receiver gives the accumulated carrier phase (also called "Doppler count"), namely, the number of cycles of the beat wave that arises due to the difference between the frequency of the incoming carrier wave and the nominal GPS L1 frequency (1575.42 MHz). If a carrier phase corresponding to a transmitter (i) is obtained by the movable antenna and stationary antenna in a unit of time (Δt), and carrier-phase values obtained by those antennas are respectively defined as $\Delta\phi_M^i(t)$ and $\Delta\phi_S^i(t)$, the phase difference between them, $\Delta\phi_{MS}^i(t)$, is represented as

$$\begin{aligned}\Delta\phi_{MS}^i(t) &= \Delta\phi_M^i(t) - \Delta\phi_S^i(t) \\ &= (\delta f + \delta F^i + f_{dop}^i)\Delta t - (\delta f + \delta F^i)\Delta t + \varepsilon_\phi \\ &= f_{dop}^i \Delta t + \varepsilon_\phi\end{aligned} \quad (1)$$

where δf and δF^i are, respectively, the receiver-frequency bias and transmitter-frequency bias, f_{dop}^i is the Doppler shift produced by the movement of the movable antenna, and ε_ϕ is observation error. To convert Eq. (1) to the unit of length, it is multiplied by the wavelength of the GPS L1 carrier wave, λ_{L1} (190.3 mm). It follows that

$$d^i(t) = \lambda_{L1}\Delta\phi_{MS}^i(t) = \lambda_{L1} f_{dop}^i \Delta t + \varepsilon_d \,. \quad (2)$$

This $d^i(t)$ is called the "delta pseudorange" in a similar manner

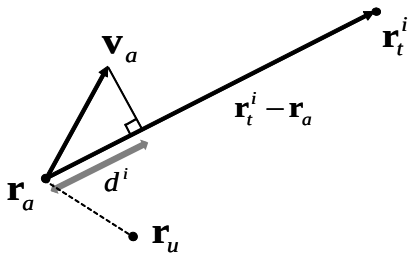

Figure 2. Vector diagram for position of a movable antenna and its velocity, transmitter position, user's position, and observed delta pseudorange in the RCS.

to that in the terminology of GPS.

C. Position calculation

Equation (2) can be modeled by using a vector expression of the geometric relation between the transmitter antennas and movable receiver antenna in the RCS. A vector diagram for each element used for position and orientation calculation is shown in Fig. 2, where the position of the movable receiver antenna is $\mathbf{r}_a$, the position of ith IMES transmitter is $\mathbf{r}_t^i$, the velocity of the movable antenna is $\mathbf{v}_a$, the observed delta pseudorange corresponding to transmitter i is d^i, which is obtained from Eq. (2), and the receiver's position to be determined is $\mathbf{r}_u$. From the geometric relationship depicted in this figure,

$$d^i = \mathbf{v}_a \cdot \frac{\mathbf{r}_t^i - \mathbf{r}_a}{\left\| \mathbf{r}_t^i - \mathbf{r}_a \right\|} + \varepsilon_d \,, \tag{3}$$

Here,

$$\mathbf{v}_a = {}^r\mathbf{R}_l \, {}^l\mathbf{v}_a \tag{4}$$

and

$$\mathbf{r}_a = \mathbf{r}_u + {}^r\mathbf{R}_l \, {}^l\mathbf{r}_a \,, \tag{5}$$

where ${}^r\mathbf{R}_l$ is the rotation matrix from the LCS to the RCS, and ${}^l\mathbf{v}_a$ and ${}^l\mathbf{r}_a$ are the velocity and position of the movable antenna in the LCS, which are obtained from the encoder attached to the rotation axis.

The coordinate system used by the proposed method follows the right-hand rule, and the rotation matrix with Euler angles is expressed as

$${}^r\mathbf{R}_l = \begin{bmatrix} C_\theta C_\phi & C_\theta S_\phi S_\psi - C_\psi S_\theta & S_\theta S_\psi + C_\theta C_\psi S_\phi \\ C_\phi S_\theta & C_\theta C_\psi + S_\theta S_\phi S_\psi & C_\psi S_\theta S_\phi - C_\theta S_\psi \\ -S_\phi & C_\phi S_\psi & C_\phi C_\psi \end{bmatrix}. \tag{6}$$

where C and S means sine and cosine, respectively, θ represents orientation (azimuth) of the receiver, and φ and ψ are inclinations (elevation) of the receiver (φ and ψ are obtained from the attitude sensor). Substituting Eqs. (4) and (5) into Eq. (3) gives

$$d^i = {}^r\mathbf{R}_l \, {}^l\mathbf{v}_a \cdot \frac{\mathbf{r}_t^i - {}^r\mathbf{R}_l \, {}^l\mathbf{r}_a - \mathbf{r}_u}{\left\| \mathbf{r}_t^i - {}^r\mathbf{R}_l \, {}^l\mathbf{r}_a - \mathbf{r}_u \right\|} + \varepsilon_d \,. \tag{7}$$

This equation is referred to hereafter as the "observation equation" of the proposed Doppler positioning method.

Equation (7) includes four unknown variables: the three-dimensional receiver's position $\mathbf{r}_u$=(x, y, and z) and orientation θ. In the same way as GPS, these variables are determined by using a non-linear least-square method (Newton-Raphson method) with a redundant set of the observation equations obtained while the receiver's antenna was moving. Here, if the four unknown variables are expressed as $\mathbf{x}$=(x, y, z, and θ) as a whole, the non-linear term of Eq. (7) is defined as

$$F(\mathbf{x}) = {}^r\mathbf{R}_l \, {}^l\mathbf{v}_a \cdot \frac{\mathbf{r}_t^i - {}^r\mathbf{R}_l \, {}^l\mathbf{r}_a - \mathbf{r}_u}{\left\| \mathbf{r}_t^i - {}^r\mathbf{R}_l \, {}^l\mathbf{r}_a - \mathbf{r}_u \right\|}. \tag{8}$$

Its partial derivatives with respect to $\mathbf{r}_u$ and θ are respectively

$$\frac{\partial F(\mathbf{x})}{\partial \mathbf{r}_u} = -\frac{({}^r\mathbf{R}_l \, {}^l\mathbf{v}_a)^T}{\left\| \mathbf{r}_t^i - {}^r\mathbf{R}_l \, {}^l\mathbf{r}_a - \mathbf{r}_u \right\|} + \frac{({}^r\mathbf{R}_l \, {}^l\mathbf{v}_a)^T (\mathbf{r}_t^i - {}^r\mathbf{R}_l \, {}^l\mathbf{r}_a - \mathbf{r}_u)(\mathbf{r}_t^i - {}^r\mathbf{R}_l \, {}^l\mathbf{r}_a - \mathbf{r}_u)^T}{\left\| \mathbf{r}_t^i - {}^r\mathbf{R}_l \, {}^l\mathbf{r}_a - \mathbf{r}_u \right\|^3} \tag{9}$$

and

$$\frac{\partial F(\mathbf{x})}{\partial \theta} = \frac{-({}^r\mathbf{R}_l \, {}^l\mathbf{v}_a)^T ({}^r\mathbf{R}'_l \, {}^l\mathbf{r}_a) + (\mathbf{r}_t^i - {}^r\mathbf{R}_l \, {}^l\mathbf{r}_a - \mathbf{r}_u)^T ({}^r\mathbf{R}'_l \, {}^l\mathbf{v}_a)}{\left\| \mathbf{r}_t^i - {}^r\mathbf{R}_l \, {}^l\mathbf{r}_a - \mathbf{r}_u \right\|} + \frac{({}^r\mathbf{R}_l \, {}^l\mathbf{v}_a)^T (\mathbf{r}_t^i - {}^r\mathbf{R}_l \, {}^l\mathbf{r}_a - \mathbf{r}_u)(\mathbf{r}_t^i - {}^r\mathbf{R}_l \, {}^l\mathbf{r}_a - \mathbf{r}_u)^T ({}^r\mathbf{R}'_l \, {}^l\mathbf{r}_a)}{\left\| \mathbf{r}_t^i - {}^r\mathbf{R}_l \, {}^l\mathbf{r}_a - \mathbf{r}_u \right\|^3}, \tag{10}$$

where ${}^r\mathbf{R}'_l$ is the partial derivative of ${}^r\mathbf{R}_l$ with respect to θ.

If the initial value of the solution of $\mathbf{x}$ is described as $\mathbf{x}_0$= (x_0, y_0, z_0, and θ_0), and if the second- and higher-order terms of the Taylor expansion of $F(\mathbf{x}_0)$ are ignored, the first updated solution of the Newton-Raphson method is represented as

$$F(\mathbf{x}_1) \approx \frac{\partial F(\mathbf{x}_0)}{\partial \mathbf{x}_0} \Delta \mathbf{x}_0 + F(\mathbf{x}_0) \,. \tag{11}$$

Equation (7) is therefore modified to

$$\begin{aligned} d^i &= F(\mathbf{x}_1) + \varepsilon_d \\ &\approx \frac{\partial F(\mathbf{x}_0)}{\partial \mathbf{x}_0}\Delta\mathbf{x}_0 + F(\mathbf{x}_0) + \varepsilon_d \end{aligned}. \quad (12)$$

Here, if the receiver acquires signals from m transmitters for n epochs of time, $m \times n$ modified observation equations (Eq. (12)) are obtained and can be expressed in the following matrix form:

$$\begin{bmatrix} \frac{\partial F_0^{1,1}}{\partial x_0} & \frac{\partial F_0^{1,1}}{\partial y_0} & \frac{\partial F_0^{1,1}}{\partial z_0} & \frac{\partial F_0^{1,1}}{\partial \theta_0} \\ \vdots & & & \\ \frac{\partial F_0^{m,n}}{\partial x_0} & \frac{\partial F_0^{m,n}}{\partial y_0} & \frac{\partial F_0^{m,n}}{\partial z_0} & \frac{\partial F_0^{m,n}}{\partial \theta_0} \end{bmatrix} \begin{bmatrix} \Delta x_0 \\ \Delta y_0 \\ \Delta z_0 \\ \Delta \theta_0 \end{bmatrix} = \begin{bmatrix} d^{1,1} - F_0^{1,1} \\ \vdots \\ d^{m,n} - F_0^{m,n} \end{bmatrix} + \boldsymbol{\varepsilon}_d . \quad (13)$$

The matrix on the left-hand side of Eq. (13) is defined as **G**, called "geometry matrix" in GPS terminology, and the column vector on the right-hand side is defined as **b**. Equation (13) is then expressed as

$$\mathbf{G}\Delta\mathbf{x}_0 = \mathbf{b} + \boldsymbol{\varepsilon}_d . \quad (14)$$

If the estimated value of $\Delta\mathbf{x}_0$ is denoted as $\Delta\hat{\mathbf{x}}_0$, the solution to Eq. (14) is given as

$$\Delta\hat{\mathbf{x}}_0 = \left(\mathbf{G}^T\mathbf{G}\right)^{-1}\mathbf{G}^T\mathbf{b} . \quad (15)$$

The estimated position is then updated iteratively according to

$$\hat{\mathbf{x}}_1 = \mathbf{x}_0 + \Delta\hat{\mathbf{x}}_0 \quad (16)$$

After this updating process is repeated several times, a sufficient approximate solution for the user's position and orientation, $\hat{\mathbf{x}}$, is acquired. Note that in the present work, since the receiver antenna rotates in a horizontal plane, z is omitted from the variables to be solved because the number of linearly independent vectors of **G** is three (two-dimensional plane plus one orientation).

D. Dilution of precision

Dilution of precision (DOP) is defined in the same manner as the previous Doppler-positioning method [5] and GPS [6]. If it is assumed that bias error of ε_d in Eq. (12) is zero, and its variance is defined as σ_d^2, the covariance matrix of $\Delta\mathbf{x}$ is given as

$$\mathrm{cov}(\Delta\mathbf{x}) = \sigma_d^{\,2}\left(\mathbf{G}^T\mathbf{G}\right)^{-1} . \quad (17)$$

If $(\mathbf{G}^T\mathbf{G})^{-1}$ is defined as **H**, DOP is expressed as the diagonal elements of **H**, where

$$\mathbf{H} = \begin{bmatrix} XDOP^2 & \bullet & \bullet & \bullet \\ \bullet & YDOP^2 & \bullet & \bullet \\ \bullet & \bullet & ZDOP^2 & \bullet \\ \bullet & \bullet & \bullet & AZDOP^2 \end{bmatrix} . \quad (18)$$

Here, "XDOP" means the DOP for the x-coordinate (likewise, the y- and z-coordinates) and "AZDOP" is an abbreviation of "azimuth DOP" for the DOP for orientation. It follows from Eqs. (17) and (18) that the variance of positioning error for each x-, y-, and z-coordinate and the variance of orientation error are given by

$$\sigma_x^2 = \sigma_d^2 XDOP^2 , \quad (19)$$

$$\sigma_y^2 = \sigma_d^2 YDOP^2 , \quad (20)$$

$$\sigma_z^2 = \sigma_d^2 ZDOP^2 , \quad (21)$$

and

$$\sigma_\theta^2 = \sigma_d^2 AZDOP^2 . \quad (22)$$

Equations (19)–(22) show that as the value of DOP increases, the variances of the estimated position and orientation also increase. If the DOP for the x-y plane is defined as HDOP,

$$HDOP^2 = XDOP^2 + YDOP^2 . \quad (23)$$

Moreover, if the standard deviation of the estimated position on the x-y plane, σ_{xy}, is defined as

$$\sigma_{xy} = \sqrt{\sigma_x^2 + \sigma_y^2} , \quad (24)$$

it follows from Eqs. (19), (20), (23), and (24) that σ_{xy} is expressed as

$$\sigma_{xy} = \sigma_d HDOP , \quad (25)$$

and it follows from Eq. (22) that

$$\sigma_\theta = \sigma_d AZDOP . \quad (26)$$

Eqs. (25) and (26) indicate that if the geometric relation between the antennas of the transmitters and the receiver are known, the precision of positioning and orientation estimation can be deduced.

III. Problems with Using Magnetic Compass

Before describing a positioning experiment with the proposed method, to clarify the importance of the orientation estimation introduced in the present work, the problems that arise when a magnetic compass is used in the previous method are explained. When the absolute orientation of the receiver on the Earth is acquired by using a magnetic compass, two errors should be considered: magnetic declination and magnetic deviation. The former is the difference between the angles of the Earth's true north and magnetic north (to which the magnetic compass directs); and the latter is angle variation due to electric devices and objects containing iron-based material.

Magnetic declination is basically bias error caused by deposits such as iron ore and magnetite inside the Earth. The information about its distribution can be obtained from government websites or so. Its value varies over time and with place, but the amount of variation is not so large. From the hourly data taken over the 31 days of October 2011 at the Kanozan Geodetic Observatory in Japan [8], the standard deviation of its time variation is 0.026 degrees, and the difference between its maximum and minimum values is 0.158 degrees. As for the variation with place, the output of a declination calculator provided by the Geospatial Information Authority of Japan [8] gives declination values with a precision of 0.017 (1/60) degrees. It is thus concluded that magnetic declination is not a source of large error in orientation measurement.

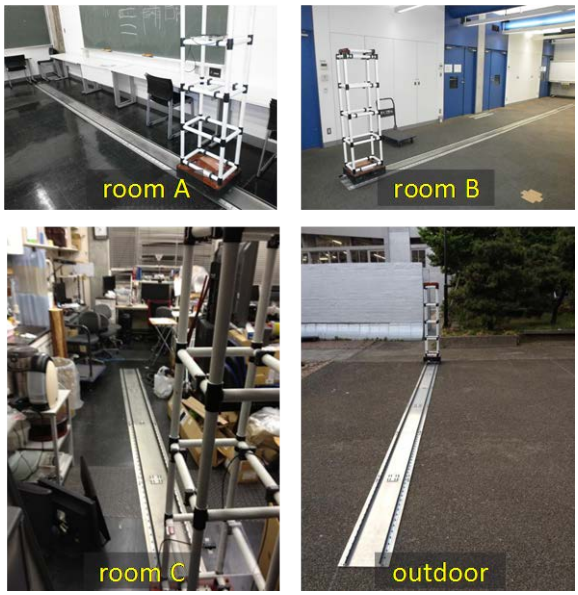

Figure 3. Orientation-measurement locations: rooms A, B, and C and outdoors.

On the other hand, magnetic deviation gives large error, especially indoors, not only because numerous electric devices and objects made of iron-based materials are present everywhere but also because buildings themselves are made of steel-reinforced concrete. In the next subsection, it is shown that the orientation of the receiver in a typical room (under the assumption that bias error is negligible) varies considerably.

A. *Variation of output from magnetic compass*

Orientation values output from a magnetic compass were obtained in three different rooms (for convenience, called "A", "B", and "C", hereafter) and outdoors as a reference (Fig. 3). For each room, the orientations on two to four straight lines were measured by using a wagon moving on rails. For each line, orientation values were obtained at ten points, with an interval of about one-twelfth of the room width, and at two different heights, referred to as "high" (130 cm) and "low" (60 cm). In the case of the outdoor measurements, the length of

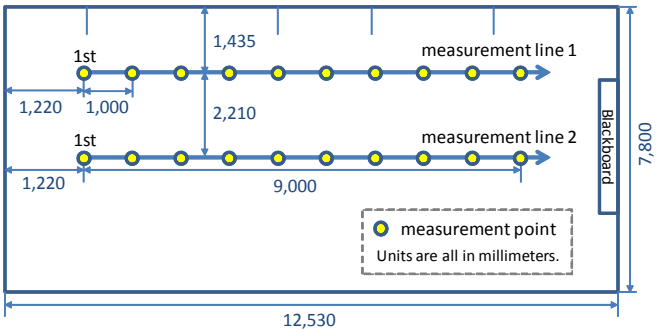

Figure 4. Measurement points in room B.

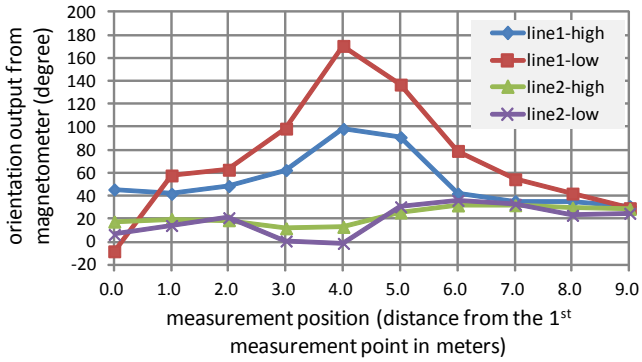

Figure 5. Orientation output from magnetic compass in room B.

TABLE I. RESULTS OF ORIENTATION MEASUREMENT (STANDARD DEVIATION FOR EACH MEASUREMENT LINE)

	room A	room B	room C	outdoor
line1-high	6.6	23.6	3.4	0.9
line1-low	5.3	52.1	1.6	1.0
line2-high	4.9	7.6	8.4	1.0
line2-low	3.3	13.3	11.0	1.3
line3-high	2.4	-	-	-
line3-low	4.2	-	-	-
line4-high	2.9	-	-	-
line4-low	6.6	-	-	-
average	4.5	24.2	6.1	1.1

Units are all in degrees.

measurement line was set to five meters. For each point on a line, orientation values were gathered for one minute and averaged. The magnetic compass (attitude sensor) used was a 3DM-GX3®-25 from MicroStrain Inc.

The measurement points and measurement results for room B, as an example of widely varying orientation, are respectively shown in Figs. 4 and 5. As shown in Fig. 5, the measured orientation value on line 1 in room B (which corresponds to the upper right photo in Fig. 3) varies by over 180 degrees. However, as seen in the photo of room B, there are no objects around the measurement line. In such a case, there is probably a power line under the floor that influences the local magnetic field. Orientations measured at each place are compared in Table I. The figures in each cell represent the standard deviation of measurements at ten points on the corresponding measurement line. As clear from the table, the orientation output from the magnetic compass varies much more indoors than it does outdoors.

B. Positioning error induced by orientation error

Orientation error included in θ of Eq. (6) induces positioning error (error included in $\hat{\mathbf{x}}$ of Eq. (16)). To estimate the magnitude of positioning error caused by orientation error, the law of propagation of errors [7] is applied to the position calculation process mentioned in Section II-C. However, since the relation between position and orientation is complex (because of the high-nonlinearity of the equations for position calculation), it is difficult to directly calculate the propagated positioning error; the relation between position and orientation is therefore simplified here as

$$x = D\cos(\theta), \tag{27}$$

$$y = D\sin(\theta), \tag{28}$$

where x and y are the coordinates of a receiver position on the x-y plane (horizontal plane), D is the distance between a transmitter and the receiver on the x-y plane (which can be calculated from Doppler observables and inclinations obtained from an accelerometer), and θ is the orientation of the receiver (which is obtained from a magnetic compass).

If the standard deviation of x, y, D, and θ are respectively represented as σ_x, σ_y, σ_D, and σ_θ, applying the law of error propagation to Eqs. (27) and (28) gives

$$\sigma_x^2 = \left(\frac{\partial x}{\partial D}\right)^2 \sigma_D^2 + \left(\frac{\partial x}{\partial \theta}\right)^2 \sigma_\theta^2, \tag{29}$$

$$\sigma_y^2 = \left(\frac{\partial y}{\partial D}\right)^2 \sigma_D^2 + \left(\frac{\partial y}{\partial \theta}\right)^2 \sigma_\theta^2. \tag{30}$$

If positioning error on the x-y plane is denoted as σ_{xy}, it follows from Eqs. (27) – (30) that

$$\sigma_{xy} = \sqrt{\sigma_x^2 + \sigma_y^2} = \sqrt{\sigma_D^2 + D^2\sigma_\theta^2}\ . \tag{31}$$

Here, if D is set to 3,000 mm, for example, according to the positioning result in a previous experiment (shown in Fig. 11 of [5]), σ_D is 171 mm. In this case, if σ_θ is 1 degree (π/180 radians), σ_{xy} is 179 mm. In the case of room B (σ_θ=0.422 radians (24.2 degrees, from Table I)), σ_{xy} becomes 1,279 mm.

As described above, orientation error induced by a magnetic compass is large and, as a result, positioning error becomes large. This means that use of a magnetic compass should be avoided.

IV. POSITIONING EXPERIMENT

A positioning experiment was conducted to evaluate the proposed Doppler positioning method. Particularly, the influence of the distance between two transmitters on the accuracy of estimated position and orientation was investigated.

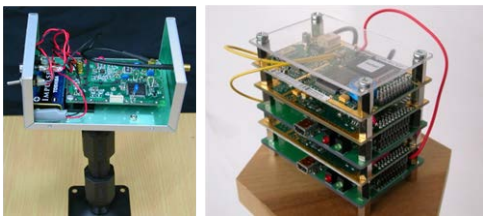

Figure 6. IMES transmitter (left) and synchronized receiver modules (right).

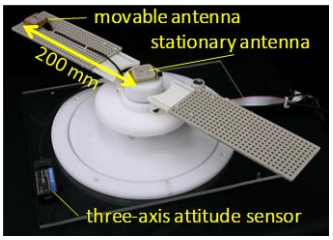

Figure 7. Doppler measurement unit.

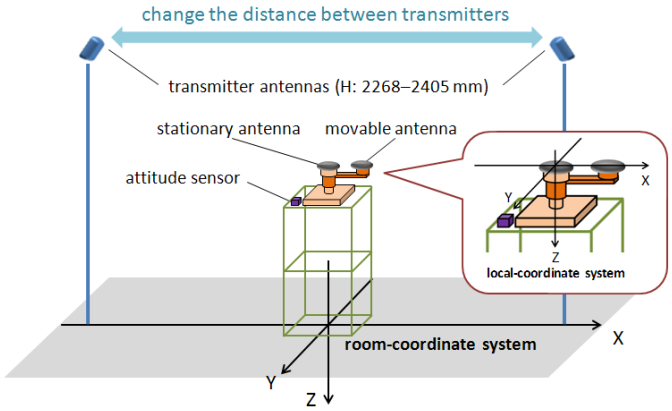

Figure 8. Experimental setup.

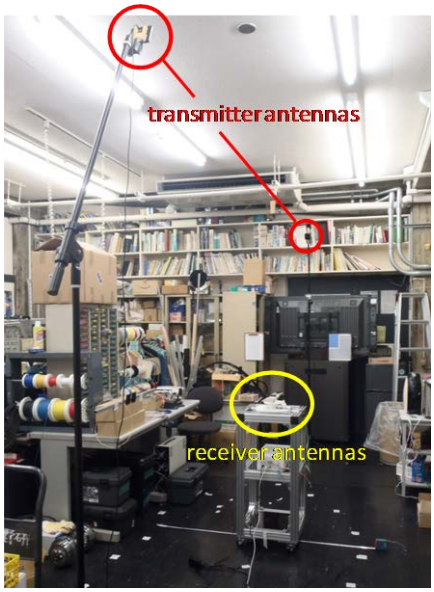

Figure 9. Overview of experimental field.

A. Devices

The IMES transmitter, synchronized receiver modules, and a Doppler measurement unit used in the positioning experiment are shown in Figs. 6 and 7. The transmitter transmits an IMES signal (C/A code modulated on the GPS L1 band), and the receiver is composed of two GPS/IMES receiver modules synchronized by a common external clock. As the receiver module, SUPERSTAR II™ from NovAtel Inc. was used with modification to its firmware. The Doppler measurement unit rotates the bar mounted on it clockwise or counterclockwise through a maximum of 360 degrees at a rotation velocity of 4 rpm. As for the attitude sensor, a 3DM-GX3R-25 from MicroStrain Inc. was used.

B. Setup and procedure

The experimental setup and overview of the experimental field are shown in Figs. 8 and 9, respectively. The position of the receiver (i.e., center of the LCS) was set to (0, 0, and −743) (all in millimeters), and the receiver's attitude was aligned by hand so that the directions of the LCS corresponded to those of the RCS; accordingly estimated orientation could be evaluated. The position and orientation of the receiver was fixed during the experiment. Transmitter antennas were installed above the x-axis (at a height of 2268–2405 mm) with the same distance between each antenna and the receiver. (The reason that antenna height has a certain range is that in order to obtain enough transmitting power, the front faces of transmitter antennas were manually adjusted in the direction of the receiver's position according to the distance between transmitter antennas.)

The experimental procedure is as follows. First, for each of ten distances between transmitter antennas (100, 250, 500, 1000, 1500, 2000, 2500, 3000, 3500, and 4000 mm), Doppler shift, position and velocity of the movable antenna in the LCS, and inclination of the receiver are measured. For each measurement, the movable antenna is rotated 360 degrees clockwise and counterclockwise until it has completed ten round trips; two-dimensional position and orientation of the receiver in the RCS, both for each round trip and all ten round trips, are then estimated by using the above-mentioned algorithm.

After the estimation process is complete, the standard deviations of the ten estimated positions and orientations for each separation distance between transmitter antennas are compared to the ideal values computationally simulated with Eqs. (25) and (26). In these equations, σ_d values of 2, 4, and 6 mm were arbitrarily used in consideration of the σ_d values, i.e., 2.9 mm (static state) and 5.2 mm (moving state), measured in a previous experiment (Section IV-C of [5]).

C. Results

Position-estimation error (i.e., difference between estimated position and true position) on the x-y plane, calculated from the square-root of the errors of the x- and y-coordinates ($Error_{xy} = \sqrt{Error_x^2 + Error_y^2}$) for each distance between transmitter antennas, is plotted in Fig. 10, where small dots indicate estimation error for each round trip, and large circles represent the error for all ten round trips. As seen in the graph, variance of position estimation error for each round trip increases as the distance between transmitter antennas increases; however, the error for ten round trips stays at almost the same level (basically less than 100 mm) regardless of the distance.

Error in estimated orientation (i.e., orientation error) is shown in Fig. 11. Except for transmitter-antenna separation distances of 100 and 250 mm, orientation error is largely within ±3 degrees; in these cases, variance of orientation error is also a little larger than that of other cases

Actual standard deviation of estimated position and orientation are compared with theoretical values derived from Eqs. (25) and (26) in Figs. 12 and 13. As can be seen in these graphs, actual values are largely in accordance with the plotted theoretical values; however, whereas actual values in Fig. 12 are mostly close to the theoretical values in the case of σ_d of 4 mm, those in Fig. 13 are below the curve for σ_d of 2 mm.

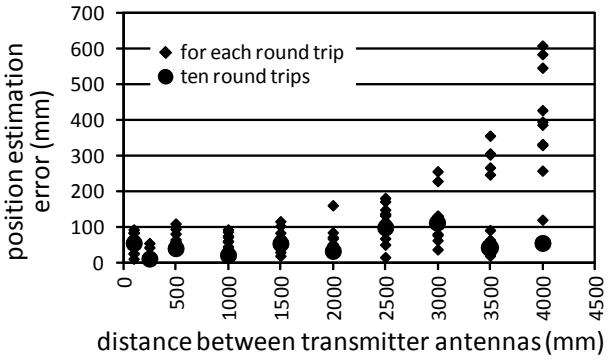

Figure 10. Position-estimation error (square-root of errors of x- and y-coordinates) for each measurement.

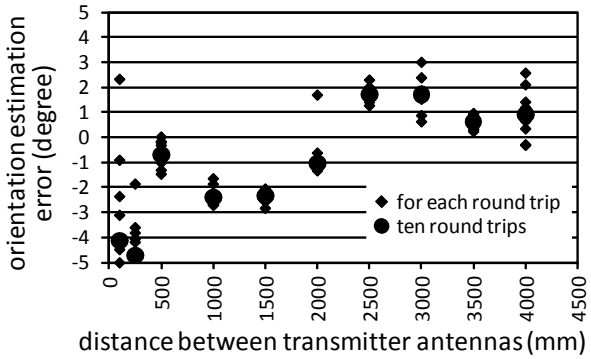

Figure 11. Orientation-estimation error for each measurement.

V. Discusion of Experimental Results

As seen in Fig. 10, centimeter- to decimeter-level positioning accuracy was basically achieved in this positioning experiment, although variance of estimated position is large in the case of a greater distance between transmitter antennas. On the other hand, the orientation accuracy was largely within ±3 degrees as shown in Fig. 11. If this orientation value is used for positioning when the number of visible transmitters becomes one (i.e., when orientation cannot be estimated), this orientation error (±3 degrees) propagates to positioning error, as mentioned in Section III-B; in this case, according to Eq. (31), positioning error becomes ±232 mm (σ_D=171 mm, D=3,000 mm).

In any case, positioning with less-than-decimeter-level error was achieved in spite of the messy environment (where there are a lot of objects) shown in Fig. 9. However, in this experiment, the antenna's direction was always adjusted to the receiver's position manually as mentioned in Section IV-B. In a practical use, the directionality pattern of antennas needs to be carefully considered according to installation environments.

As shown in the comparison between the values of standard deviation of estimated position and orientation and their theoretical values depicted in Figs. 12 and 13, the standard deviation of orientation estimation is less than that of position estimation. This reason is unclear for now but probably geometric error in the actual experimental setup (such as pose bias and phase center shifts of the transmitters' and receiver's

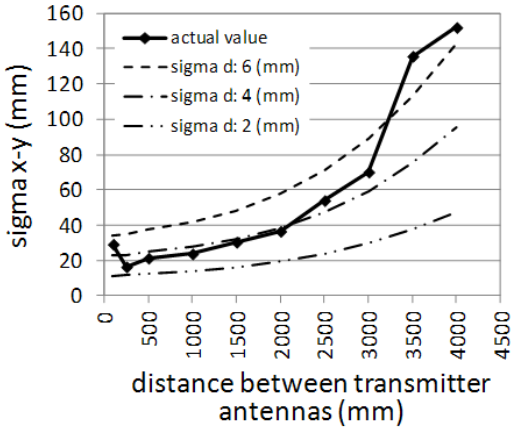

Figure 12. Comparison between standard deviations of estimated position obtained from experiment (solid line) and their theoretical values calculated by simulation (dashed line).

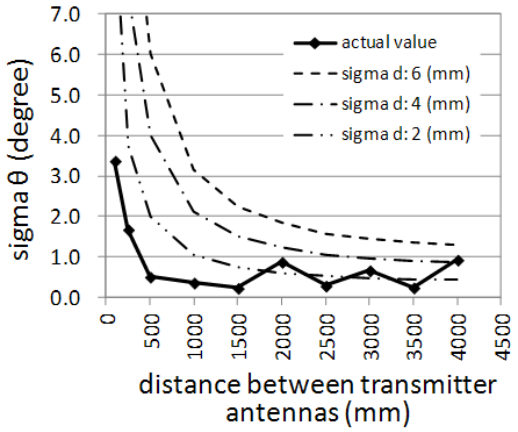

Figure 13. Comparison between standard deviations of estimated orientation obtained from experiment (solid line) and their theoretical values calculated by simulation (dashed line).

antennas) affects the position estimation more than orientation estimation.

The reason that the standard deviation of position and orientation estimation varies according to the distance between transmitter antennas is intuitively explained. At first, the case of position estimation (Fig. 12) is discussed. When the distance between the transmitter and receiver antennas increases, the ring-like trajectory of the receiver's movable antenna becomes visually small from the transmitter antenna's viewpoint. If the distance becomes large, the trajectory of the movable antenna looks like not a circle but a single point. In that case, positional difference on the antenna's trajectory is buried and lost in the error of the Doppler observable in Eq. (7); as a result, positioning error becomes large. This explanation also applies to the case that the rotation radius of the movable antenna is small (see Fig. 10 of [5]). In the case of orientation estimation (Fig. 13), if the distance between transmitter antennas decreases and ultimately becomes zero, there is no clue to determine the orientation because the number of transmitter antennas becomes virtually one. That is the reason that orientation error becomes exponentially larger when the distance between transmitter antennas becomes very small.

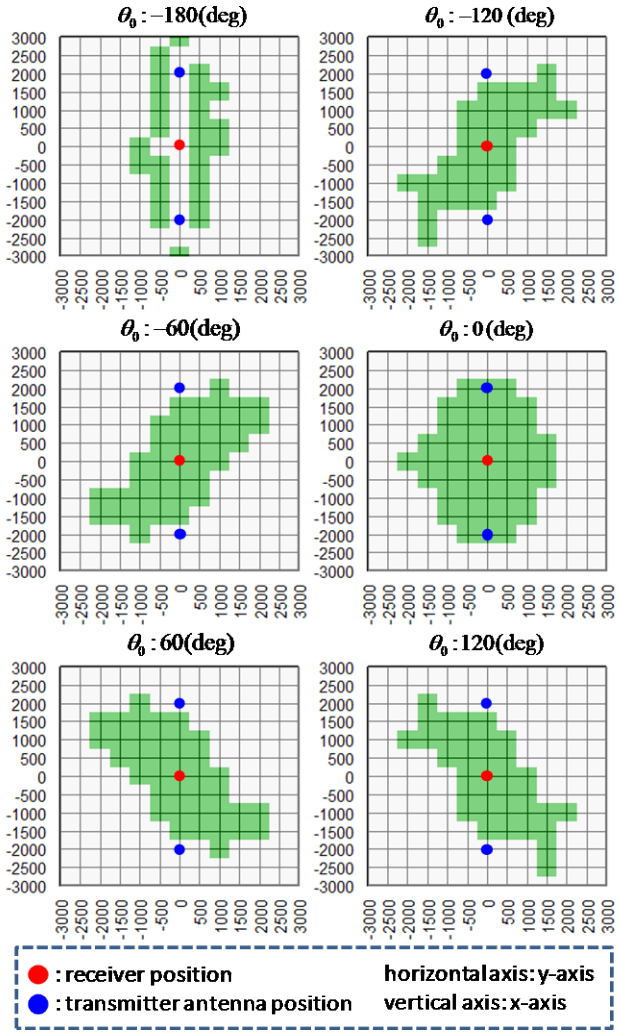

Figure 14. Initial values that converge on correct estimation results (green area).

VI. Initial-Value Analysis

As mentioned in Section II-C, the observation equation used for position and orientation estimation is nonlinear, and the nonlinear least-squares based on the Newton-Raphson method is used to solve them. In this case, whether or not a right estimation result is acquired depends on the initial value of the iterative calculation by the Newton-Raphson method ($\mathbf{x}_0$ in Eq. (16)). Which initial values converge to appropriate position and orientation are determined as follows. At first, the experimental data (Doppler shifts, velocity and position of the movable receiver antenna, etc.) of ten round trips with transmitter-antenna separation distance of 2,000 mm is used. The position and orientation of the receiver are estimated under the condition that the initial values of x_0, y_0, and θ_0 are varied by intervals of 500 mm, 500 mm, and 60 degrees, respectively, in the range of $-3{,}000 \le x_0 \le 3{,}000$ (mm), $-3{,}000 \le y_0 \le 3{,}000$ (mm), and $-180 \le \theta_0 \le 180$ (degrees). For each estimation, if the estimated values after ten iterations (x_{10}, y_{10}, and θ_{10}) are converged within x_{best}±10 mm, y_{best}±10 mm, and θ_{best}±1 degrees, the estimated value is regarded as the appropriate one. (x_{best}, y_{best}, and θ_{best} respectively represent the best-estimated x- and y-coordinates and orientation of the receiver, whose values are 33.3 mm, 0.9 mm, and −0.99 degrees, of all values estimated with the selected data.)

The initial values that converged to the right estimation results are illustrated in Fig. 14. Green areas mean initial values that converged to an appropriate value. Red and blue circles respectively mean the position of the receiver and transmitter antenna. As shown in the graph, if the initial position is set to around the midst of two transmitters (i.e., x_0 =0 and y_0=0), the initial values converge to an appropriate value, except in the case that initial orientation (θ_0) is −180 degrees (upper-left graph). This result implies that if the estimation is repeated several times with different initial orientation values while the initial position is set at the midst of two transmitters, position and orientation of the receiver can be estimated appropriately. However, in the present work, the midmost position of two transmitters happened to be the same as the receiver's position. Accordingly, initial-value analysis with various receiver positions is a future work.

VII. Concluding Remarks

Position estimation with centimeter- to decimeter-level accuracy and orientation estimation within ±3 degrees were achieved by using the proposed Doppler positioning method with two IMES transmitters. Moreover, it was shown that the accuracy of position and orientation estimation depends on the separation distance between transmitter antennas, and it can be estimated theoretically by using the concept of DOP. These results will provide hints for making a guideline for IMES transmitter installation (e.g., "For estimating orientation of robots, two transmitters near an entrance should be installed at two-meter interval.").

References

[1] Japan Aerospace Exploration Agency (JAXA) Interface Specification for QZSS ver.1.4, http://qz-vision.jaxa.jp/USE/is-qzss/index_e.html

[2] Naohiko Kohtake, Shusuke Morimoto, Satoshi Kogure, and Dinesh Manandhar, "Indoor and Outdoor Seamless Positioning using Indoor Messaging System and GPS," 2011 International Conference on Indoor Positioning and Indoor Navigation (IPIN2012), Sep. 2011

[3] S. Cobb, "GPS pseudolites: Theory, design, and applications," Ph.D. Thesis, Stanford University, 1997

[4] M. O. Kanli, "Limitations of pseudolite systems using off-the-shelf GPS receivers," in *Proc. of Int. Symposium. on GNSS/GPS*, Sydney, Australia, Dec. 2004.

[5] Yoshihiro Sakamoto, Hiroaki Arie, Takuji Ebinuma, Kenjiro Fujii, and Shigeki Sugano, "High-Accuracy IMES Localization Using a Movable Receiver Antenna and a Three-axis Attitude Sensor," 2011 International Conference on Indoor Positioning and Indoor Navigation (IPIN2012), Sep. 2011

[6] R.B. Langley, "Dilution of Precision," GPS World, Vol. 10, No. 5, pp.52-9, May 1999.

[7] Propagation of uncertainty, Wikipedia, http://en.wikipedia.org/wiki/Propagation_of_uncertainty

[8] Geospatial Information Authority of Japan, http://vldb.gsi.go.jp/sokuchi/geomag/index-e.html